

Investigation of Ga Doping for Non-stoichiometric Sodium Bismuth Titanate Ceramics

minyan Li

Yan'an University

chan he

Yan'an University

weiguo wang (✉ wwgissp@126.com)

Yan'an University <https://orcid.org/0000-0002-1067-168X>

gangling hao

Yan'an University

xianyu li

Yan'an University

ting liu

Yan'an University

xinfu wang

Yan'an University

dan wang

Yan'an University

Research Article

Keywords: oxygen ion conductor, $\text{Na}_{0.5}\text{Bi}_{0.5}\text{TiO}_3$, doping, internal friction, vacancy mobility

Posted Date: March 18th, 2021

DOI: <https://doi.org/10.21203/rs.3.rs-316726/v1>

License:   This work is licensed under a Creative Commons Attribution 4.0 International License.

[Read Full License](#)

Investigation of Ga doping for non-stoichiometric sodium bismuth titanate ceramics

M.Y. Li, C. He, W.G. Wang*, G. L. Hao, X.Y. Li, T. Liu, X.F. Wang, D. Wang
College of Physics and Electronic Information, Yan'an University, Yan'an 716000, P. R. China

Abstract: The electrical performance of Ga³⁺ doping Na_{0.5}Bi_{0.5}TiO₃-based oxygen ion conductor was studied. The Na_{0.52}Bi_{0.47}Ti_{1-x}Ga_xO_{3-δ} (x=0, 0.01, 0.015, 0.02) samples were fabricated by the means of traditional solid-state reaction. The results of AC impedance measurement show that the bulk conductivity of Na_{0.52}Bi_{0.47}Ti_{1-x}Ga_xO_{3-δ} samples decrease monotonously with the increase of Ga³⁺ doping. At 673 K, the bulk conductivity of the Na_{0.52}Bi_{0.47}Ti_{0.98}Ga_{0.02}O_{3-δ} sample is 7.19×10⁻⁴ S/cm, which is lower than that of Na_{0.52}Bi_{0.47}TiO_{3-δ} sample under the identical test temperature. The highest total conductivity emerges in the Na_{0.52}Bi_{0.47}Ti_{0.99}Ga_{0.01}O_{3-δ} sample with 1.387×10⁻⁴ S/cm at 623 K for the Ga³⁺ doping content of 1 mol%, which demonstrate that a slight of Ga³⁺ doping supports the enhancement of the total conductivity. A relaxation peak was observed in the Na_{0.52}Bi_{0.47}Ti_{1-x}Ga_xO_{3-δ} compounds. As the Ga³⁺ ions were introduced into the Na_{0.52}Bi_{0.47}TiO_{3-δ} compound, there is an increasing trend of the relaxation activation energy deduced by the internal friction test. In addition, the oxygen relaxation height of Na_{0.52}Bi_{0.47}Ti_{1-x}Ga_xO_{3-δ} samples decreases along with the introduction of the Ga³⁺ doping, suggesting that the introduction of the Ga³⁺ leads to the decrease of mobile oxygen vacancy .

Keywords: oxygen ion conductor; Na_{0.5}Bi_{0.5}TiO₃; doping; internal friction; vacancy mobility

1. Introduction

Oxygen ion conductors have been quite broadly used, such as oxygen pumps, oxygen separation membranes and solid oxide fuel cells (SOFC), etc.[1-6]. In the past several decades, there are multitudinous research groups devoting to study oxygen ion

* Corresponding author, Tel: +86-911-2650504; Fax: +86-911-2650504, E-mail: wwgissp@126.com

conductors[1-3]. Recently, $\text{Na}_{0.5}\text{Bi}_{0.5}\text{TiO}_3$ (NBT), a ferroelectric material with perovskite structure[7,8], can be found that there is a large leakage conductivity. According to the Li et al. experimental results, the leakage conductivity results from the migration of oxygen defect in the NBT compounds. The oxygen defect mainly comes from the loss of the low melting point elements during preparation [6,9]. It is worthy mentioning that the bulk conductivity can reach 1×10^{-2} S/cm at the temperature of 873 K for the 2 mol% Mg^{2+} doped bismuth-deficient NBT compound, $\text{Na}_{0.5}\text{Bi}_{0.49}\text{Ti}_{0.98}\text{Mg}_{0.02}\text{O}_{2.965}$ [1,7]. The experimental result offers a new option for exploring intermediate-temperature oxygen ion conductors.

To get the higher electrical properties in the NBT based oxygen ion conductors, higher oxygen vacancy content is necessary. There are two ways to introduce oxygen vacancies into NBT compound: Bi- deficiency and acceptor doping[10]. According to Li Ming et al. results[6], the ionic conductivity can be greatly improved through introducing a low-level non-stoichiometric defect(<1 at.%) in NBT[1,7]. Especially, the compositions containing Bi-deficient or Na excess exhibit 3-4 orders of magnitude higher than the compositions with Na-deficient or Bi excess[11]. For the other way of introducing oxygen vacancies, it mainly focuses on the acceptor doping of A or B sites. A site acceptor doping are mainly on the trivalent Bi^{3+} ions replaced by the monovalent ions (Li^+ , Na^+ , K^+) or divalent ions (Ca^{2+} , Sr^{2+} , Ba^{2+})[1,7,13]. Yang et al. Reported that Sr^{2+} doped Bi-deficient NBT-based compounds ($\text{Na}_{0.5}\text{Bi}_{0.47}\text{Sr}_{0.02}\text{TiO}_{2.975}$) is a profitable means to improve the electrical properties for oxygen ion conductors[14]. The B-site doping mainly concentrate on low valent ions such as Mg^{2+} , Ga^{3+} for Ti^{4+} [1-3]. From the Li et al. experimental results[6], it can be found that the bulk conductivity of the Mg^{2+} doped bismuth-deficient NBT-based compounds ($\text{Na}_{0.5}\text{Bi}_{0.49}\text{Mg}_{0.02}\text{Ti}_{0.98}\text{O}_{2.965}$) which designed by the above two methods is higher than that of the stable ZrO_2 doped with 8mol% Y_2O_3 [1,6]. Xu et al. have investigated that the impact of K^+ and Ga^{3+} co-doped on the electric properties of NBT based oxygen ion conductor[2]. In our previous work, we have introduced excess Na^+ in NBT-based oxygen ion conductor, the bulk conductivity of $\text{Na}_{0.54}\text{Bi}_{0.46}\text{TiO}_{2.96}$ is 1.6×10^{-3} S/cm at 673 K[15]. Considering that the ionic radius of

Ga^{3+} (0.062 nm) is very close to that of Ti^{4+} (0.061 nm) leading to a small elastic strain energy which is beneficial to the formation of stable solid solution[1-2], Ga^{3+} ion was selected as a acceptor ion to substitute the B-site Ti^{4+} ions included the Bi-deficient $\text{Na}_{0.52}\text{Bi}_{0.47}\text{TiO}_{3-\delta}$ compound to gain the higher electrical properties of NBT oxygen ion conductors. The phase structure, electrical properties and diffusion of oxygen ions were studied by X-ray diffractometer, impedance spectrum and internal friction spectrum respectively.

2 Experimental procedure

The $\text{Na}_{0.52}\text{Bi}_{0.47}\text{Ti}_{1-x}\text{Ga}_x\text{O}_{3-\delta}$ compounds ($x=0, 0.01, 0.015, 0.02$) were elaborated by conventional solid phase reaction method using high purity Na_2CO_3 , Bi_2O_3 , TiO_2 and Ga_2O_3 [13]. In order to eliminate absorbed water and CO_2 , the raw materials mentioned above were dried at 573 K for around 12 h. The detailed preparation procedure can be seen in Ref. [12]. The initial reactive $\text{Na}_{0.52}\text{Bi}_{0.47}\text{Ti}_{1-x}\text{Ga}_x\text{O}_{3-\delta}$ powders were compacted into the cylindrical and bar samples, then the compacted samples were sintered at 1323 K for 12 h with the same compositions $\text{Na}_{0.52}\text{Bi}_{0.47}\text{Ti}_{1-x}\text{Ga}_x\text{O}_{3-x}$ powder embedded around them.

The phase structure of $\text{Na}_{0.52}\text{Bi}_{0.47}\text{Ti}_{1-x}\text{Ga}_x\text{O}_{3-\delta}$ samples was detected by a laboratory X-ray diffractometer (Japanese Science Ultima IV diffractometer) using $\text{CuK}\alpha$ incident radiation in the range of $10^\circ \leq 2\theta \leq 80^\circ$. The conductive silver paste was well-distributed applied on the upper and lower surfaces of the cylinder sample and baked at 973 K for 2 h to serve as an electrode. In order to study the electrical performance of the samples, the impedance spectroscopy technique was applied using Impedance Analyzer instrument (Instrument type: IM 3536, 10–8 MHz) with a frequency range of 1 Hz to 1 MHz from 473 K to 723 K . The low- frequency internal friction (IF) spectroscopy were performed on a inverted torsion pendulum in the form of forced vibration controlled by a computer.

3 Experimental results

3.1 Phase structure

Figure 1 shows the XRD patterns of $\text{Na}_{0.5}\text{Bi}_{0.5}\text{TiO}_3$ and $\text{Na}_{0.52}\text{Bi}_{0.47}\text{Ti}_{1-x}\text{Ga}_x\text{O}_{3-\delta}$ ($x=0, 0.01, 0.015, 0.02$) samples. There were no extra peaks of impurity phase in the

compositions of Na⁺ excess and Ga³⁺ doped NBT samples through comparing the diffraction pattern with Na_{0.5}Bi_{0.5}TiO₃ compound, which suggested that excess Na⁺ and Ga³⁺ ions are dissolved into the perovskite lattice of NBT-based compounds[13]. According to Scherrer equation: $D=K\lambda/\beta\cos\theta$, where D is the grain sizes, K is the Scherrer constant (generally 0.89), β is the full width at half maximum (FWHM) of the diffraction peak, and 2θ is the diffraction angle, the grain sizes is inversely proportional to the FWHM[3]. From the XRD patterns of Na_{0.52}Bi_{0.47}Ti_{1-x}Ga_xO_{3-δ} samples, it can be obtained that the FWHM of the the diffraction peak ($2\theta=32.8^\circ$) for Na_{0.52}Bi_{0.47}Ti_{1-x}Ga_xO_{3-δ} ($x=0, 0.01, 0.015, 0.02$) samples are $0.366^\circ, 0.481^\circ, 0.387^\circ$ and 0.369° , respectively. Thus, it can be deduced that the grain size of Na_{0.52}Bi_{0.47}Ti_{0.99}Ga_{0.01}O_{3-δ} ($x=0.01$) sample is smallest.

For perovskite structure materials, Goldschmidt tolerance factor t is of great significance to the structural stability and properties[17]. By the definition of the Goldschmidt tolerance factor, The tolerance factor of the Na_{0.52}Bi_{0.47}Ga_xTi_{1-x}O_{3-δ} ($x=0, 0.01, 0.015, 0.02$) samples are 0.97662, 0.97658, 0.97654 and 0.97652, separately. The tolerance factor for the Na_{0.52}Bi_{0.47}Ti_{1-x}Ga_xO_{3-δ} ($x=0, 0.01, 0.015, 0.02$) samples was virtually unchanged, which indicates that Ga³⁺ doping has very little effects on the lattice distortion.

3.2 Ionic conductivity

Figure 2 represents the complex impedance spectra for the Na_{0.52}Bi_{0.47}Ti_{1-x}Ga_xO_{3-δ} ($x=0, 0.01, 0.015$) samples at 643 K. Considering the image recognition, the plot of the Na_{0.52}Bi_{0.47}Ti_{0.98}Ga_{0.02}O_{3-δ} sample is not given. The complex impedance spectra of the Na_{0.52}Bi_{0.47}Ti_{1-x}Ga_xO_{3-δ} samples all contain three depressed semicircles, in which the semicircles at high frequency and low frequency correspond to grain polarization and electrode polarization response. And the depressed semicircles locating at the intermediate-frequency range can be ascribed to the grain boundary response[18]. An equivalent circuit formed by three R//CPE elements in series is used to fit the impedance spectrum[16,19]. The curve-fitting results are presented in the table 1. The capacitance at high frequency and low

frequency is about 10^{-10} F and 10^{-7} F, which is the typical grain response and electrode response of oxygen ion conductor[12,13,19].

The conductivity of $\text{Na}_{0.52}\text{Bi}_{0.47}\text{Ti}_{1-x}\text{Ga}_x\text{O}_{3-x}$ ($x=0, 0.01, 0.015, 0.02$) samples can be obtained by the formula $\sigma = L/(SR)$, in which L and S refer to the bottom area and the thickness of cylinder sample, respectively. The bulk conductivity and total conductivity can be calculate by $\sigma_b = L/(SR_b)$ and $\sigma_t = L/(SR_t)$, where R_t is the total resistance of the sum of grain resistance and grain boundary resistance[3,19]. Figure 3 exhibits the Arrhenius plots of the bulk conductivity for the $\text{Na}_{0.52}\text{Bi}_{0.47}\text{Ti}_{1-x}\text{Ga}_x\text{O}_{3-\delta}$ samples ($x=0, 0.01, 0.015, 0.02$)[15]. Because the conductivity of the $\text{Na}_{0.52}\text{Bi}_{0.47}\text{Ti}_{1-x}\text{Ga}_x\text{O}_{3-\delta}$ ($x=0, 0.01, 0.015, 0.02$) samples is very close, it's hard to distinguish them apart. Thus figure 4 exhibits the bulk conductivity of $\text{Na}_{0.52}\text{Bi}_{0.47}\text{Ti}_{1-x}\text{Ga}_x\text{O}_{3-\delta}$ samples dependent the Ga^{3+} doping content. Unlike other doped elements, the bulk conductivity of the $\text{Na}_{0.52}\text{Bi}_{0.47}\text{Ti}_{1-x}\text{Ga}_x\text{O}_{3-\delta}$ ($x=0, 0.01, 0.015, 0.02$) samples presents a monotonous reduction with the increase of Ga^{3+} concentration[1]. When the Ga^{3+} doped content increases from 1 mol% to 2 mol%, the bulk conductivity decreases from 1.01×10^{-3} S/cm to 7.19×10^{-4} S/cm at 673 K.

Figure 5 gives the total conductivity of the $\text{Na}_{0.52}\text{Bi}_{0.47}\text{Ti}_{1-x}\text{Ga}_x\text{O}_{3-x}$ samples dependent the Ga^{3+} doping content at the different measuring temperature[13,15]. With introducing Ga^{3+} into the $\text{Na}_{0.52}\text{Bi}_{0.47}\text{Ti}_{1-x}\text{Ga}_x\text{O}_{3-x}$ samples, the total conductivity shows a tendency to increase first and then decrease. When 1 mol% Ga^{3+} is introduced, the highest total conductivity can be obtained with 1.387×10^{-4} S/cm at 623 K, suggesting that a slight of Ga^{3+} doping can enhance the total conductivity of the $\text{Na}_{0.52}\text{Bi}_{0.47}\text{Ti}_{1-x}\text{Ga}_x\text{O}_{3-x}$ compounds[1]. From the analyzed results of XRD curves, there is the smaller grain size of the $\text{Na}_{0.52}\text{Bi}_{0.47}\text{Ti}_{0.99}\text{Ga}_{0.01}\text{O}_{3-\delta}$ ($x=0.01$) sample. The smaller grain size causes the larger grain boundary volume and lower impurity density in the grain boundary of the $\text{Na}_{0.52}\text{Bi}_{0.47}\text{Ti}_{0.99}\text{Ga}_{0.01}\text{O}_{3-\delta}$ ($x=0.01$) sample, which results in the lower grain boundary resistance and higher grain boundary conductivity[3]. Therefore, the grain boundary conductivity in $\text{Na}_{0.52}\text{Bi}_{0.47}\text{Ti}_{0.99}\text{Ga}_{0.01}\text{O}_{3-\delta}$ ($x=0.01$) sample is higher, which further leads to the higher total conductivity.

3.3 Internal friction spectroscopy

The temperature dependence of IF (Q^{-1}) for $\text{Na}_{0.52}\text{Bi}_{0.47}\text{Ga}_{0.015}\text{Ti}_{0.985}\text{O}_{3-\delta}$ sample at two frequency of 2 Hz and 4 Hz is exhibited in Fig.6 [13,15]. Within the test temperature range, three obvious IF peaks (entitled by P_1 around 343 K, P_2 around 543 K and P_3 around 785 K for 2 Hz) can be observed. As the test frequency increases, the peak position of P_1 peak shifts to the higher temperature, which suggests that P_1 peak has typical thermal activation relaxation characteristics[13,20]. For P_2 and P_3 peaks, the peak positions hardly move when the test frequency changes, which is the representative phase transition peak characteristic. Based on the reported research results, the P_2 and P_3 peak may result from the transition process, which correspond to the rhombohedral to orthorhombic phase and the orthorhombic to tetragonal phase, respectively[15,21].

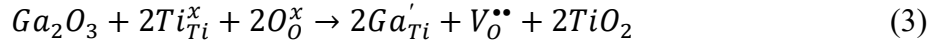
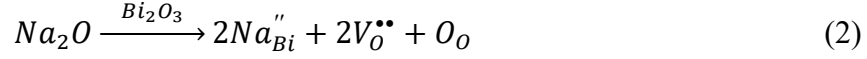
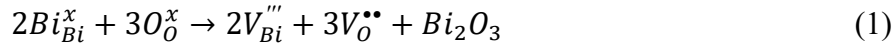
Figure 7 presents the P_1 peak curve and non-linear fitting result of $\text{Na}_{0.52}\text{Bi}_{0.47}\text{Ti}_{0.985}\text{Ga}_{0.015}\text{O}_{3-\delta}$ sample[15]. For the thermally activated relaxation process, the relation between the relaxation time τ and activation energy E can be expressed by Arrhenius law: $\tau = \tau_0 \exp(E/K_B T)$ [13,20]. By changing the tested frequency measurement, the relaxation parameters E and the relaxation time τ can be got: $E=0.78$ eV for the $\text{Na}_{0.52}\text{Bi}_{0.47}\text{TiO}_{3-\delta}$ sample[13]. It is easy to find that the activation energies of the Ga^{3+} doped $\text{Na}_{0.52}\text{Bi}_{0.47}\text{Ti}_{1-x}\text{Ga}_x\text{O}_{3-\delta}$ ($x=0.01, 0.015, 0.02$) samples range from 0.83 eV to 0.86 eV, which is higher than that of $\text{Na}_{0.52}\text{Bi}_{0.47}\text{TiO}_{3-\delta}$ sample, possibly indicating that Ga^{3+} doping is not beneficial to oxygen ion diffusion.

In order to further study the influence of Ga^{3+} introduced into NBT based oxygen ion conductor on oxygen ion diffusion, the IF curves of the $\text{Na}_{0.52}\text{Bi}_{0.47}\text{Ga}_x\text{Ti}_{1-x}\text{O}_{3-\delta}$ ($x=0, 0.01, 0.015, 0.02$) samples measured at 4 Hz with different Ga^{3+} doping concentration were shown in Fig.8. The internal friction peaks of all samples around 350 K are observed from Fig.8. Although the IF peak positions are almost unchanged, the IF peak height decrease with the increase of Ga^{3+} doping concentration, which can be found in the inset of figure 8.

4 Discussion

Through bismuth-deficient and Na/Ga acceptor doping methods, oxygen

vacancy can be introduced into NBT-based compounds just like the following Kroger-Vink equations[3,13]:



According to the principle of electric neutrality, there are 3.5 mol% nominal oxygen vacancy can be led into the $Na_{0.52}Bi_{0.47}Ti_{0.99}Ga_xO_{3-\delta}$ sample, which results from Bi^{3+} defect and Na^+ acceptor doping. Additionally, there are more 0.5 mol% oxygen vacancies introduced into the $Na_{0.52}Bi_{0.47}Ti_{0.99}Ga_{0.01}O_{3-\delta}$ compounds when the Ga doped content is 1 mol%, suggesting that oxygen vacancy concentration can be increased due to introduce Ga^{3+} into the $Na_{0.52}Bi_{0.47}Ti_{1-x}Ga_xO_{3-\delta}$ samples .

According to the reported results[12], not all oxygen vacancies are involved in the diffusion migration of oxygen ions and there are immobile oxygen vacancies in the oxygen conductor. Normally, the mobile oxygen vacancies are of great significance to the electrical properties of oxygen-ion conductors[3]. Based on the point defect relaxation theory, the height of the relaxation peak have a linear relationship with the mobile vacancy concentration[13]. The inset of figure 8 gives the peaks height of P_1 peaks for the $Na_{0.52}Bi_{0.47}Ti_{1-x}Ga_xO_{3-\delta}$ ($x = 0, 0.01, 0.015, 0.02$) compounds dependent the Ga^{3+} doping content. Obviously, the height of the P_1 peaks for $Na_{0.52}Bi_{0.47}Ti_{1-x}Ga_xO_{3-\delta}$ compounds decrease with the increase of the Ga^{3+} doping concentration. Namely, the mobile oxygen vacancy concentration decrease with the introduction of the Ga^{3+} into the $Na_{0.52}Bi_{0.47}Ti_{1-x}Ga_xO_{3-\delta}$ samples. In $Na_{0.52}Bi_{0.47}Ti_{1-x}Ga_xO_{3-\delta}$ compounds, due to electrostatic attraction, there is a capture effect between oxygen vacancy and B-site acceptor ion such as Ga^{3+} , which leads to the formation of defect pairs such as $(Ga_{Ti}' - V_O^{\bullet\bullet})^{\times}$ and $(Ga_{Ti}' - V_O^{\bullet\bullet})^{\bullet}$. The decline in mobile oxygen vacancy content as a direct consequence of the formation of defect pairs[1-2].

For the perovskite structural oxygen ion conductors, oxygen ion migration mainly passes through the Na-Bi-Ti saddle point as a rate-limiting step[7]. When Ga^{3+} ions

are introduced into the $\text{Na}_{0.52}\text{Bi}_{0.47}\text{TiO}_{3-\delta}$ compound, the polarizability of the donor ions ($\alpha_{\text{Ga}}=1.50 \text{ \AA}^3$) is lower than that of the substituted ion ($\alpha_{\text{Ti}}=2.93 \text{ \AA}^3$), which is unfavourable for oxygen vacancy transport [2]. The increase of the oxygen relaxation activation energy deduced from the IF measurement also proves that Ga^{3+} doping is not beneficial to oxygen ion diffusion in the NBT-based oxygen-ion conductors.

5 Conclusion

$\text{Na}_{0.52}\text{Bi}_{0.47}\text{Ti}_{1-x}\text{Ga}_x\text{O}_{3-\delta}$ ($x=0, 0.01, 0.015, 0.02$) samples with single perovskite phase were fabricated by the way of conventional solid-state reaction. Through the AC impedance test, a slight of Ga^{3+} doping can decrease the grain-boundary resistivity and increase the total ionic conductivity. The highest total conductivity emerges in the $\text{Na}_{0.52}\text{Bi}_{0.47}\text{Ti}_{0.99}\text{Ga}_{0.01}\text{O}_{3-\delta}$ sample with the Ga^{3+} doping content of 1 mol%, which is $1.387 \times 10^{-4} \text{ S/cm}$ at 623 K. The bulk conductivity of $\text{Na}_{0.52}\text{Bi}_{0.47}\text{Ti}_{1-x}\text{Ga}_x\text{O}_{3-\delta}$ samples exhibit a monotonous reduction. The bulk conductivity of $\text{Na}_{0.52}\text{Bi}_{0.47}\text{Ti}_{0.99}\text{Ga}_{0.01}\text{O}_{3-\delta}$ ($x=0, 0.01, 0.015, 0.02$) reaches $1.01 \times 10^{-3} \text{ S/cm}$ at 673 K declined to $7.19 \times 10^{-4} \text{ S/cm}$ for the $\text{Na}_{0.52}\text{Bi}_{0.47}\text{Ti}_{0.98}\text{Ga}_{0.02}\text{O}_{3-\delta}$ sample. Through the internal friction measurement at different frequencies, there is an increase trend of the oxygen ion relaxation activation energy along with the introduction of the Ga^{3+} , meanwhile, the mobile oxygen vacancies concentration decrease owing to the formation of local defect clusters, which is the possible reason that the bulk conductivity of $\text{Na}_{0.52}\text{Bi}_{0.47}\text{Ti}_{1-x}\text{Ga}_x\text{O}_{3-\delta}$ ($x=0, 0.01, 0.015, 0.02$) samples reduce with the Ga^{3+} doping concentration.

Acknowledgments

This work has been subsidized by the National Natural Science Foundation of China (No. 12064044, 11604286).

Reference

1. R. Bhattacharyya, S. Omar, Electrical conductivity study of Ga doped non-stoichiometric sodium bismuth titanate ceramics. *J. Alloy. Compd.* 746, 54-61 (2018)
2. X. M. Xu, X. Liu, R. R. Rao, Y. X. Zhao, H. Du, J. Shi, Electrical properties and conduction mechanisms of K, Ga co-substituted $\text{Na}_{0.5}\text{Bi}_{0.5}\text{TiO}_3$ ferroelectrics. *Ceramics.* 46(14), 2772-8842 (2020)

3. W. G. Wang, M. Y. Li, X. Y. Li, G. L. Hao, The investigation on the Sr, Mg codoped $\text{Na}_{0.5}\text{Bi}_{0.5}\text{TiO}_3$ oxide ion conductor prepared by spark plasma sintering. *Ionics*. 25, 4265-4271 (2019)
4. W. G. Wang, M. Y. Li, T. Liu, X. F. Wang, D. Wang, G. L. Hao, The effect of A-site sublattice order on the electrical properties of $\text{Na}_{0.5}\text{Bi}_{0.5}\text{TiO}_3$ compound. *J. Mater. Sci.: Mater. Electron.* 30(16), 15139-15144 (2019)
5. H. Yahiro, T. Ohuchi, K. Eguchi, Electrical properties and microstructure in the system ceria-alkaline earth oxide. *Journal of Materials Science. J. Mater. Sci.* 23, 1036-1041 (1988)
6. M. Li, M. J. Pietrowski, R. A. De Souza, H. Zhang, I. M. Reaney, S. N. Cook, J. A. Sinclair, A family of oxide ion conductors based on the ferroelectric perovskite $\text{Na}_{0.5}\text{Bi}_{0.5}\text{TiO}_3$. *Nat. Mater.* 13, 31-35 (2014)
7. F. Yang, P. Wu, D. C. Sinclair, Enhanced bulk conductivity of A-site divalent acceptor-doped non-stoichiometric sodium bismuth titanate. *Solid State Ionics* 299, 38-45(2017)
8. J. Q. Huang, F. Y. Zhu, D. Huang, B. Wang et al., Intermediate-temperature conductivity of B-site doped $\text{Na}_{0.5}\text{Bi}_{0.5}\text{TiO}_3$ -based lead-free ferroelectric ceramics. *Ceram. Int.* 42, 16798-16803(2016)
9. R. Bhattacharyya, S. Das, A. Das, S. Omar et al., Effect of sintering temperature on the microstructure and conductivity of $\text{Na}_{0.54}\text{Bi}_{0.46}\text{Ti}_{0.99}\text{Mg}_{0.01}\text{O}_{3-\delta}$. *Solid State Ionics*, 360, 115547(2021)
10. F. Yang, J. S. Dean, Q. Hu, P. Wu et al., From insulator to oxide-ion conductor by a synergistic effect from defect chemistry and microstructure: acceptor-doped Bi-excess sodium bismuth titanate $\text{Na}_{0.5}\text{Bi}_{0.51}\text{TiO}_{3.015}$. *J. Mater. Chem A* 8(2020)
11. R. Bhattacharyya, S. Omar, Influence of excess sodium addition on the structural characteristics and electrical conductivity of $\text{Na}_{0.5}\text{Bi}_{0.5}\text{TiO}_3$. *Solid State Ionics* 317, 115-121(2018)
12. W. G. Wang, X. Y. Li, T. Liu, G. L. Hao, Mechanical and dielectric relaxation studies on the fast oxide ion conductor $\text{Na}_{0.54}\text{Bi}_{0.46}\text{TiO}_{2.96}$. *Solid State Ionics* 290, 6-11(2016)
13. W. G. Wang, Study on the electrical conductivity and relaxation behavior of K-doped $\text{Na}_{0.5}\text{Bi}_{0.5}\text{TiO}_3$ ceramics. *J. Mater. Sci.: Mater. Electron.* 29, 3973-3979(2019)
14. F. Yang, H. Zhang, L. Lin, I. M. Reaney, D. C. Sinclair, High ionic conductivity with low degradation in A-site strontium doped non-stoichiometric sodium bismuth titanate perovskite. *Chem. Mater.* 28, 5269-5273 (2016)
15. W. G. Wang, X. Y. Li, T. Liu, G. L. Hao, Study on electrical Conductivity and oxygen migration of the oxide-ion conductors $\text{Na}_{0.5}\text{Bi}_{0.5}\text{Ti}_{1-x}\text{Mg}_x\text{O}_{3-x}$. *B. Mater. Sci.* 42, 1-8(2019)
16. D. P. Almond, A.R. West, Impedance and modulus spectroscopy of "real" dispersive conductors. *Solid State Ionics* 11, 57-64 (1983)
17. F. Yang, P. Wu, D. C. Sinclair, Suppression of electric conductivity and switching of conduction mechanisms in 'stoichiometric' $(\text{Na}_{0.5}\text{Bi}_{0.5}\text{TiO}_3)_{1-x}(\text{BiAlO}_3)_x$ ($0 \leq x \leq 0.08$) solid solutions. *J. Mater. Chem. C* 5, 7243-7252(2017)
18. W. G. Wang, X. Y. Li, T. Liu, G. L. Hao, Influence of A-site Off-stoichiometry on grain conductivity and oxygen relaxation behavior of $\text{Na}_{0.5}\text{Bi}_{0.5}\text{TiO}_3$ ceramics. *Solid State Ionics* 327, 117-122(2018)
19. W. G. Wang, X. P. Wang, Y. X. Gao, Q. F. Fang, Lithium-ionic diffusion and electric conduction in the $\text{Li}_7\text{La}_3\text{Ta}_2\text{O}_{13}$ compounds. *Solid State Ionics* 180, 1252-1256(2009)

20. W. G. Wang, X. P. Wang, C. Li, Y. L. Li, Q. F. Fang, Damping properties of $\text{Li}_5\text{La}_3\text{Ta}_2\text{O}_{12}$ particles reinforced aluminum matrix composites. *Mater. Sci. Eng. A* 518, 190-193(2009)
21. Y. Z. Liu, G. P. Zheng, Anelastic analyses on the relaxation of anti-ferroelectric states in $0.94\text{Na}_{0.5}\text{Bi}_{0.5}\text{TiO}_3$ - 0.06BaTiO_3 solid solutions under electric fields. *J. Electroceram.* 34(1), 38-42(2015)
22. X. P. Wang, F. Fang, Mechanical and dielectric relaxation studies on the mechanism of oxygen ion diffusion in $\text{La}_2\text{Mo}_2\text{O}_9$. *Phys. Rev. B* 65(6), 064304(2002)

Table 1 AC impedance spectra and fitting results of $\text{Na}_{0.52}\text{Bi}_{0.47}\text{Ti}_{1-x}\text{Ga}_x\text{O}_{3-\delta}$ ($x=0, 0.01, 0.015, 0.02$) samples

sample	R_b (Ω)	C_b (F)	R_{gb} (Ω)	C_{gb} (F)	R_{el} (Ω)	C_{el} (F)
$\text{Na}_{0.52}\text{Bi}_{0.47}\text{TiO}_{3-\delta}$	416	2.68810^{-10}	2111	1.67×10^{-7}	7702	5.75×10^{-6}
$\text{Na}_{0.52}\text{Bi}_{0.47}\text{Ga}_{0.01}\text{Ti}_{0.99}\text{O}_{3-\delta}$	409	2.77×10^{-10}	827.5	1.17×10^{-7}	4288	6.27×10^{-6}
$\text{Na}_{0.52}\text{Bi}_{0.47}\text{Ga}_{0.015}\text{Ti}_{0.985}\text{O}_{3-\delta}$	541	3.16×10^{-10}	1986	2.93×10^{-7}	3106	1.77×10^{-5}
$\text{Na}_{0.52}\text{Bi}_{0.47}\text{Ga}_{0.02}\text{Ti}_{0.98}\text{O}_{3-\delta}$	627	4.18×10^{-10}	1122	9.38×10^{-8}	1617	3.95×10^{-5}

Figure Captions

Fig.1 Room temperature XRD patterns for the $\text{Na}_{0.5}\text{Bi}_{0.5}\text{TiO}_3$ and $\text{Na}_{0.52}\text{Bi}_{0.47}\text{Ti}_{1-x}\text{Ga}_x\text{O}_{3-\delta}$ ($x=0, 0.01, 0.015, 0.02$) samples.

Fig.2 The AC impedance plots of the $\text{Na}_{0.52}\text{Bi}_{0.47}\text{Ti}_{1-x}\text{Ga}_x\text{O}_{3-\delta}$ ($x=0, 0.01, 0.015$) samples at 643 K.

Fig.3 The Arrhenius plots of bulk conductivity for the $\text{Na}_{0.52}\text{Bi}_{0.47}\text{Ti}_{1-x}\text{Ga}_x\text{O}_{3-\delta}$ ($x=0, 0.01, 0.015, 0.02$) samples.

Fig.4 The bulk conductivity of the $\text{Na}_{0.52}\text{Bi}_{0.47}\text{Ga}_x\text{Ti}_{1-x}\text{O}_{3-\delta}$ ($x=0, 0.01, 0.015, 0.02$) samples at the different temperature.

Fig.5 The total conductivity of the $\text{Na}_{0.52}\text{Bi}_{0.47}\text{Ti}_{1-x}\text{Ga}_x\text{O}_{3-\delta}$ ($x=0, 0.01, 0.015, 0.02$) samples at different temperature (593K, 613 K and 623 K).

Fig.6 IF Q^{-1} versus temperature for the $\text{Na}_{0.52}\text{Bi}_{0.47}\text{Ti}_{0.985}\text{Ga}_{0.015}\text{O}_{3-\delta}$ sample measured at different frequencies (2 Hz and 4 Hz) in the temperature range from room temperature to 700 K.

Fig.7 IF Q^{-1} versus temperature for the $\text{Na}_{0.52}\text{Bi}_{0.47}\text{Ti}_{0.985}\text{Ga}_{0.015}\text{O}_{3-\delta}$ sample measured at different frequencies (1 Hz, 2 Hz and 4 Hz) in the temperature range from 290 K to 425 K and non-linear fitting results.

Fig.8 IF Q^{-1} versus temperature for the $\text{Na}_{0.52}\text{Bi}_{0.47}\text{Ti}_{1-x}\text{Ga}_x\text{O}_{3-\delta}$ ($x=0, 0.01, 0.015$) samples measured at 4 Hz in the temperature range from 290 K to 440 K. The curve of the relaxation time τ versus Ga^{3+} doped content is given in the inset.

Figure 1 by M. Y. Li *et al*

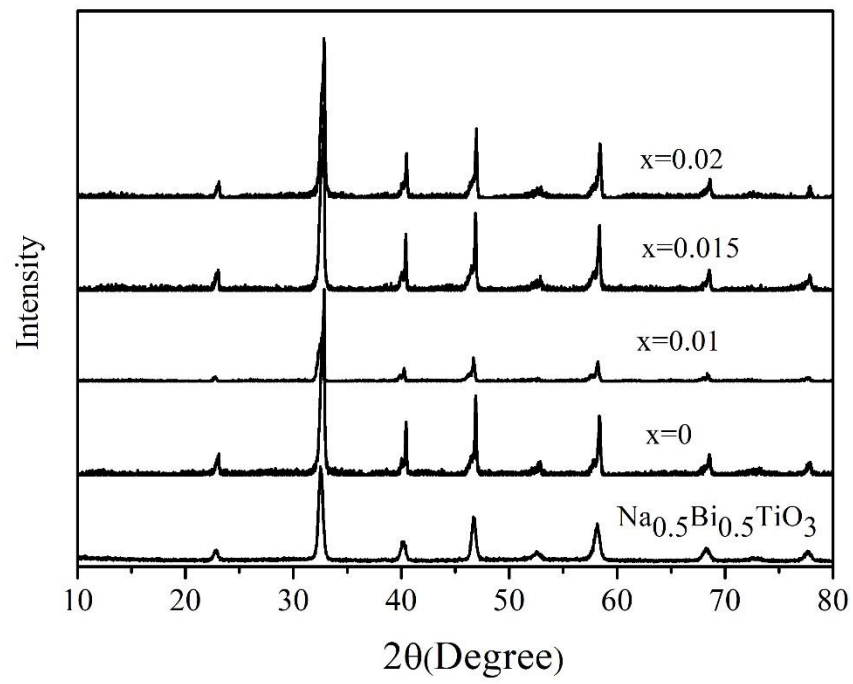


Figure 2 by M. Y. Li *et al*

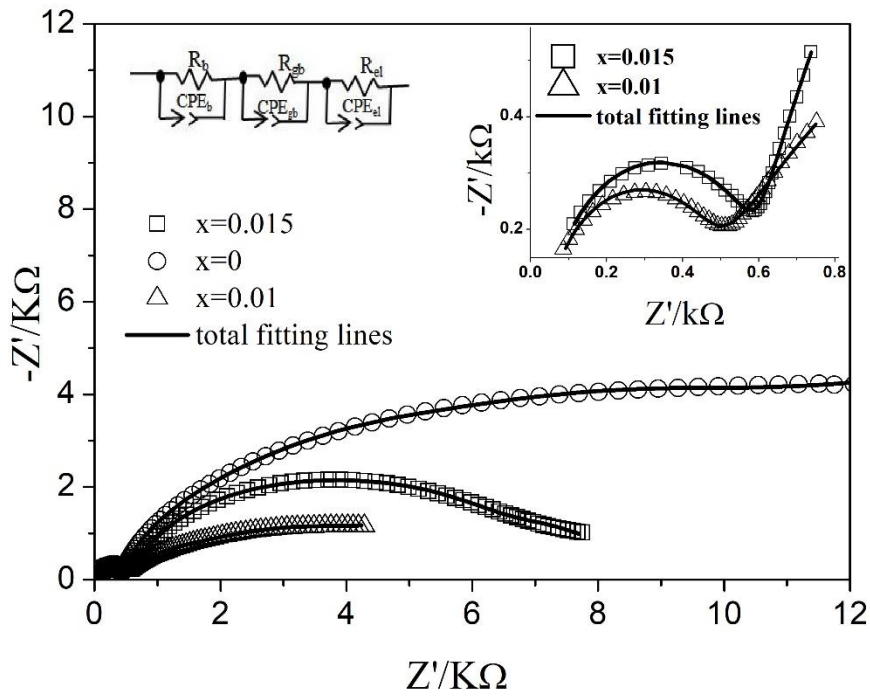


Figure 3 by M. Y. Li *et al*

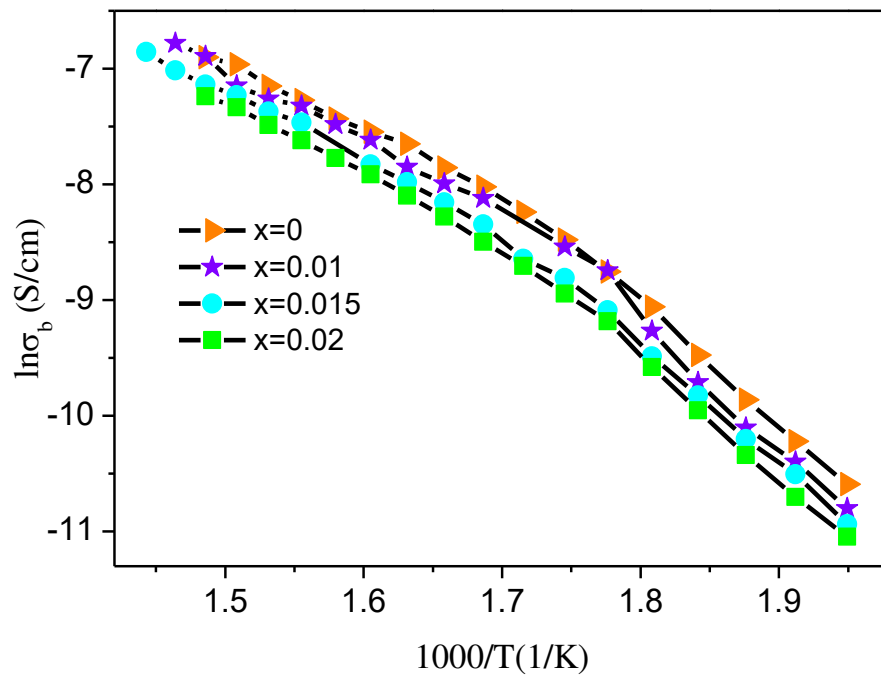


Figure 4 by M. Y. Li *et al*

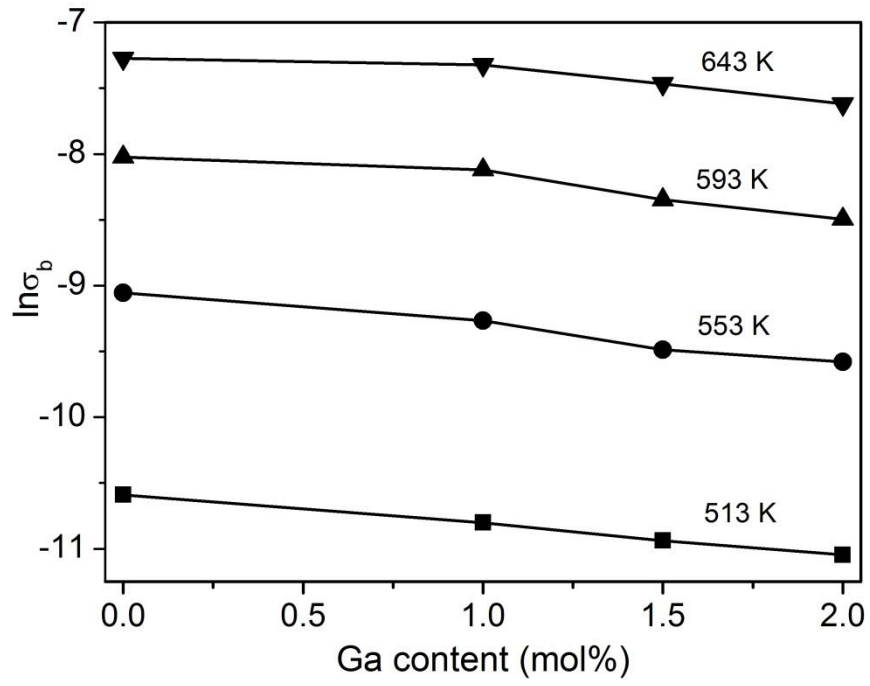


Figure 5 by M. Y. Li *et al*

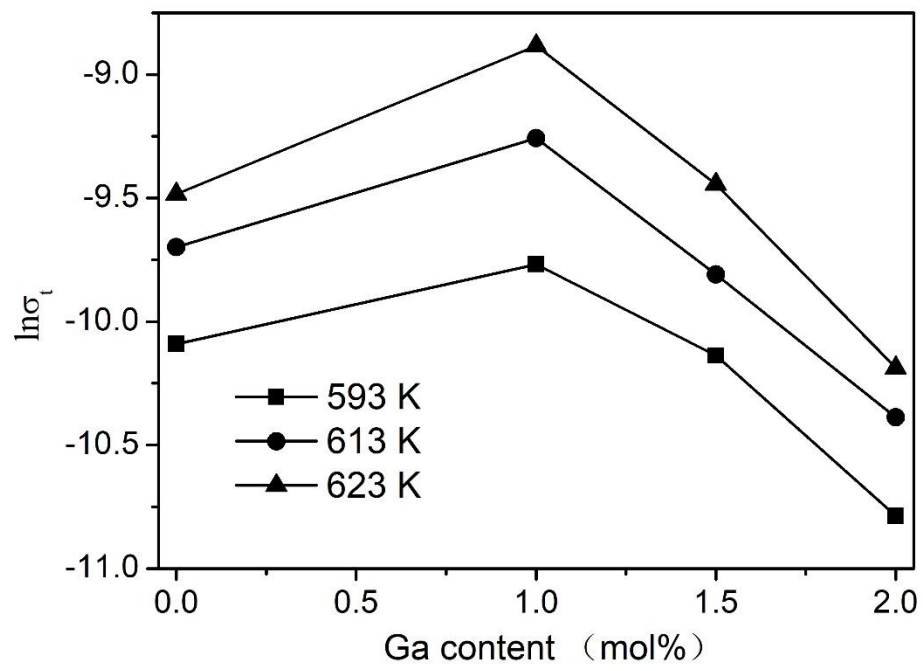


Figure 6 by M. Y. Li *et al*

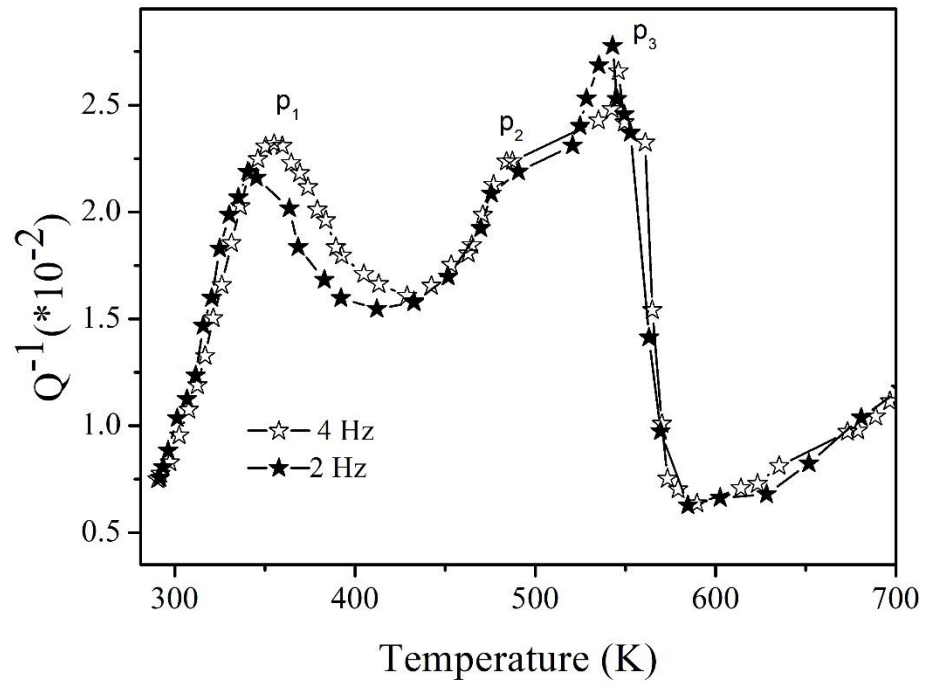


Figure 7 by M. Y. Li *et al*

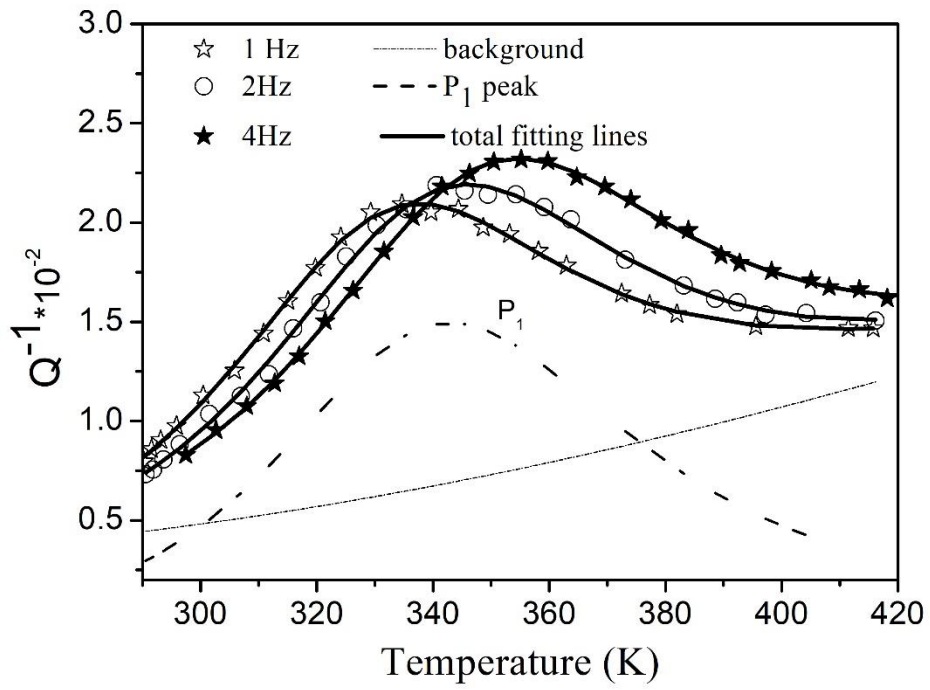
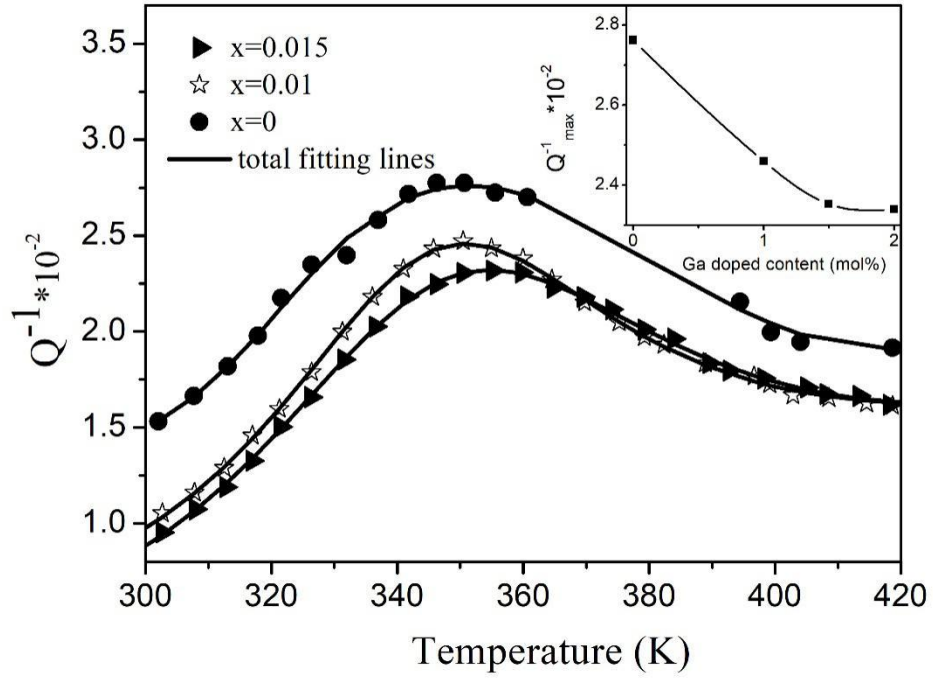


Figure 8 by M. Y. Li *et al*



Figures

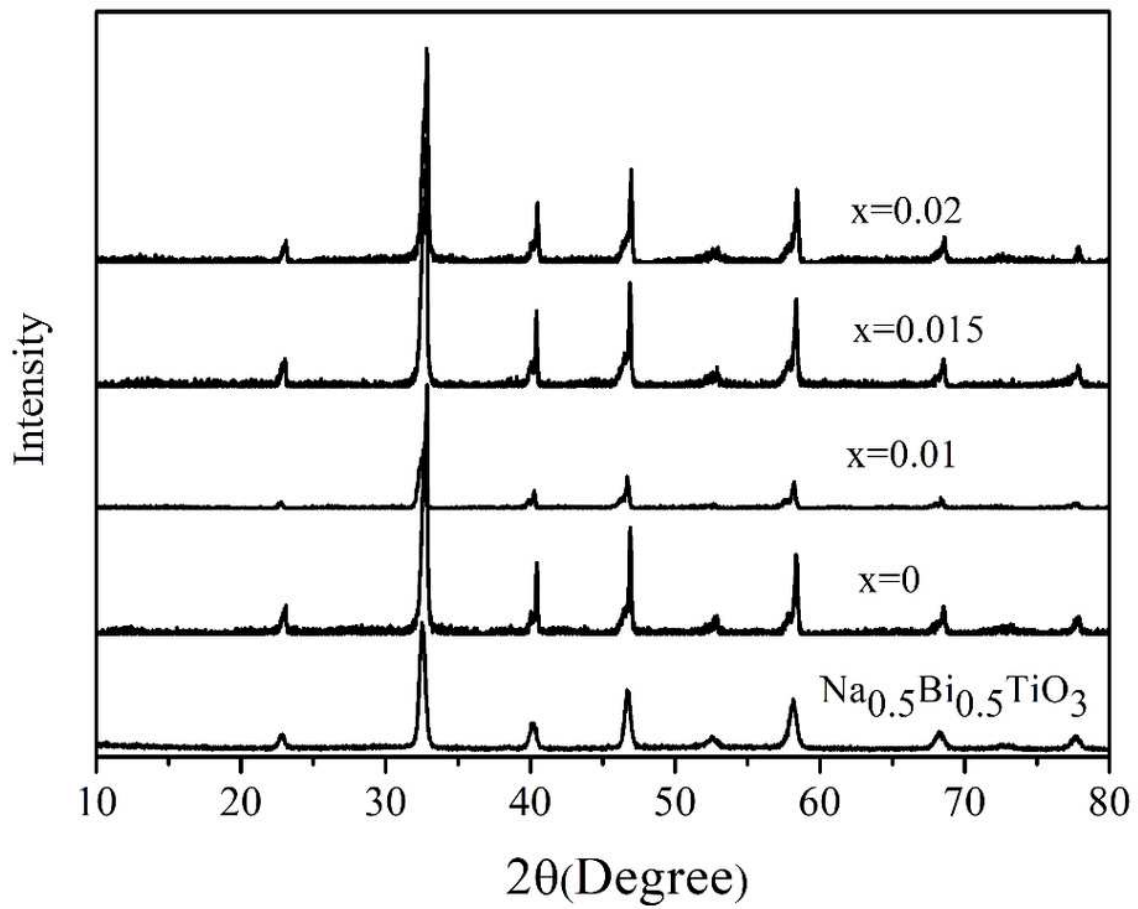


Figure 1

Room temperature XRD patterns for the $\text{Na}_{0.5}\text{Bi}_{0.5}\text{TiO}_3$ and $\text{Na}_{0.52}\text{Bi}_{0.47}\text{Ti}_{1-x}\text{Ga}_x\text{O}_{3-\delta}$ ($x=0, 0.01, 0.015, 0.02$) samples.

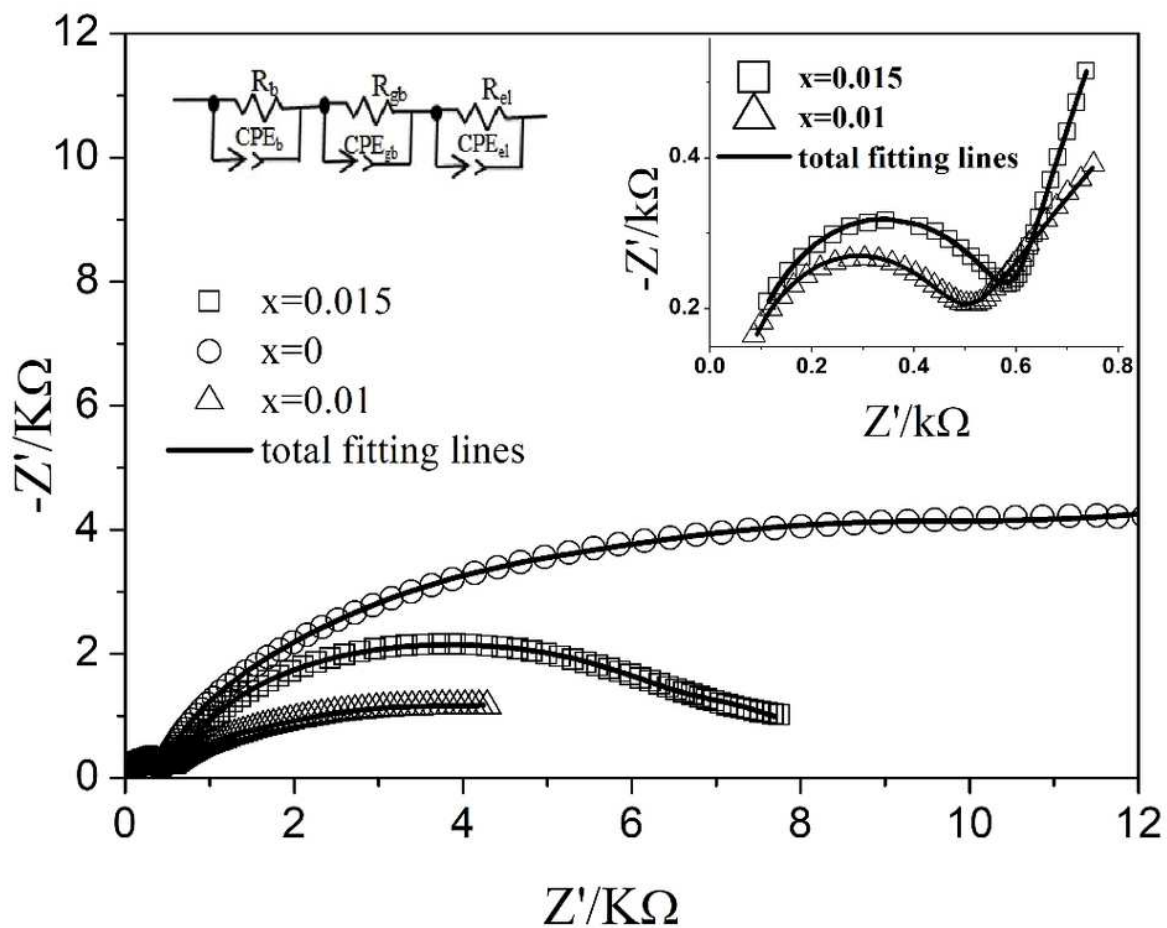


Figure 2

The AC impedance plots of the $\text{Na}_{0.52}\text{Bi}_{0.47}\text{Ti}_{1-x}\text{Ga}_x\text{O}_{3-\delta}$ ($x=0, 0.01, 0.015$) samples at 643 K.

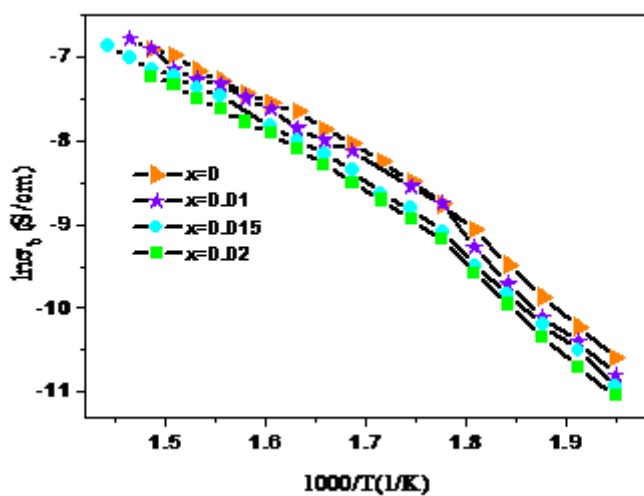


Figure 3

The Arrhenius plots of bulk conductivity for the $\text{Na}_{0.52}\text{Bi}_{0.47}\text{Ti}_{1-x}\text{Ga}_x\text{O}_{3-\delta}$ ($x=0, 0.01, 0.015, 0.02$) samples.

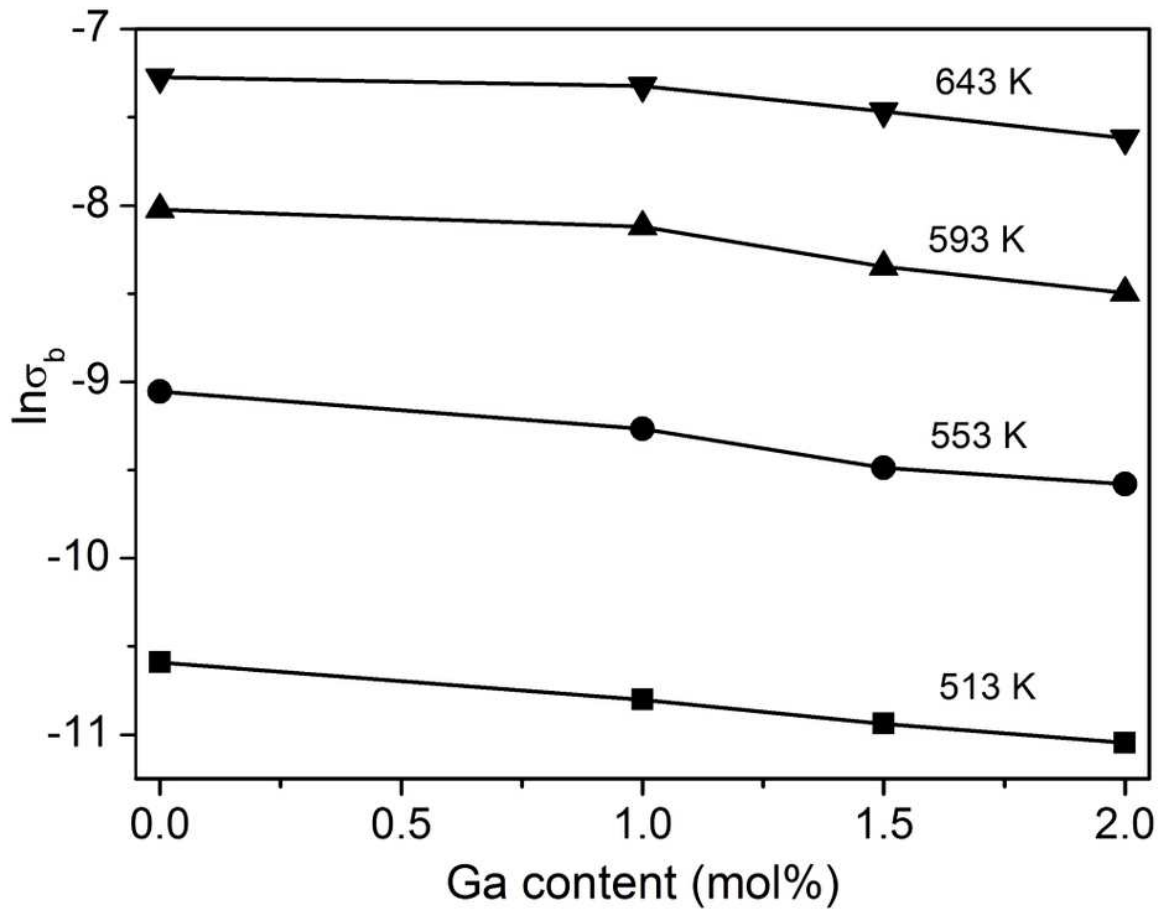


Figure 4

The bulk conductivity of the $\text{Na}_{0.52}\text{Bi}_{0.47}\text{Ga}_x\text{Ti}_{1-x}\text{O}_{3-\delta}$ ($x=0, 0.01, 0.015, 0.02$) samples at the different temperature.

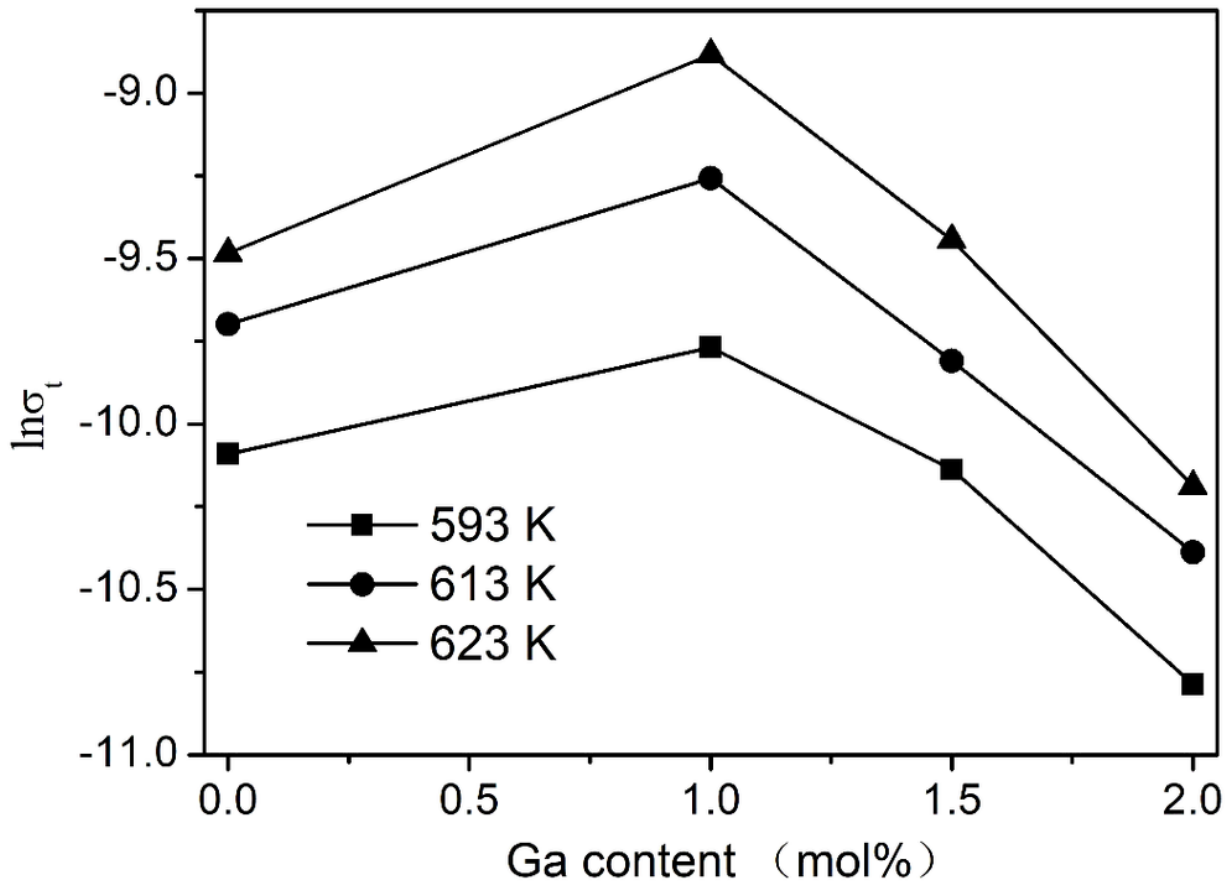


Figure 5

The total conductivity of the $\text{Na}_{0.52}\text{Bi}_{0.47}\text{Ti}_{1-x}\text{Ga}_x\text{O}_{3-\delta}$ ($x=0, 0.01, 0.015, 0.02$) samples at different temperature (593K, 613 K and 623 K).

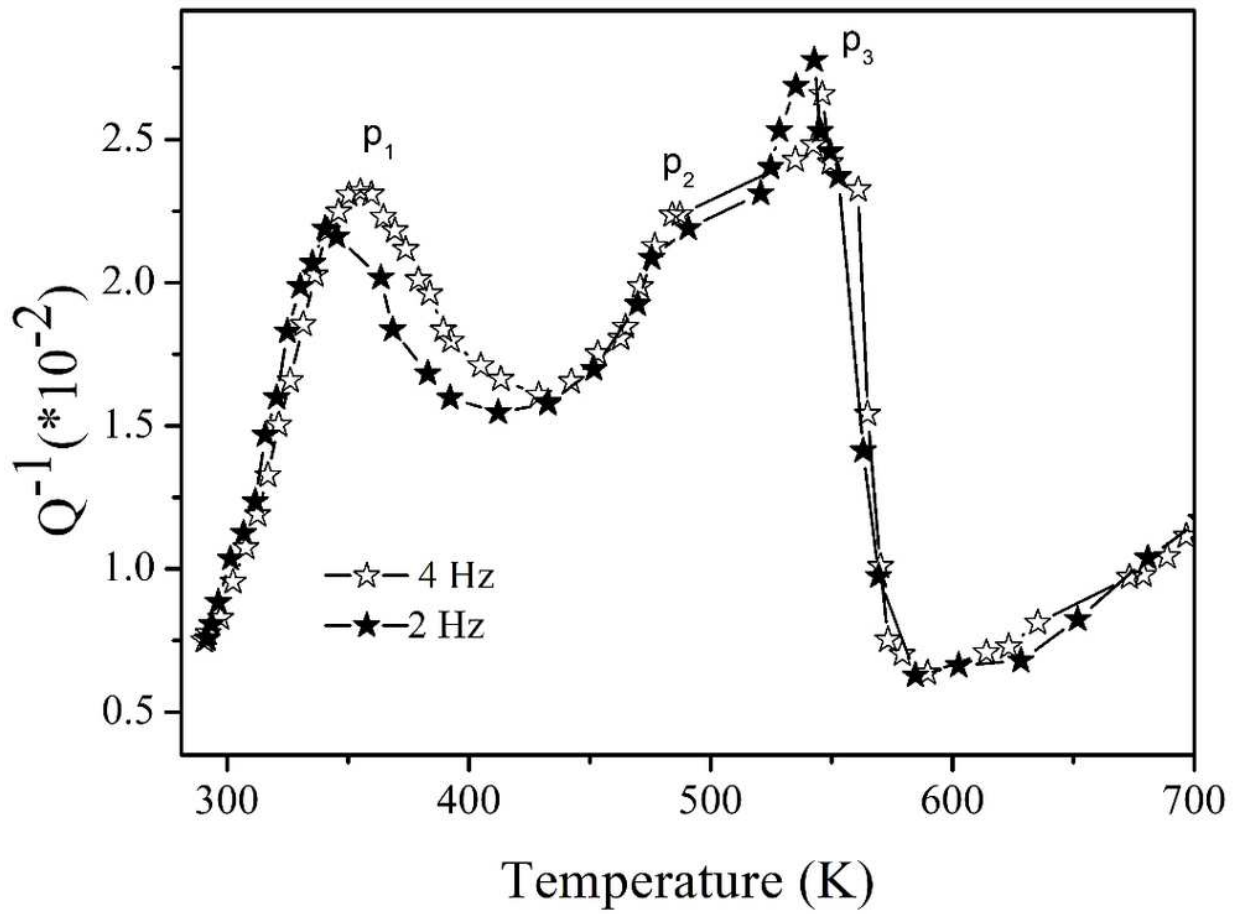


Figure 6

IF Q^{-1} versus temperature for the $\text{Na}_{0.52}\text{Bi}_{0.47}\text{Ti}_{0.985}\text{Ga}_{0.015}\text{O}_{3-\delta}$ sample measured at different frequencies (2 Hz and 4 Hz) in the temperature range from room temperature to 700 K.

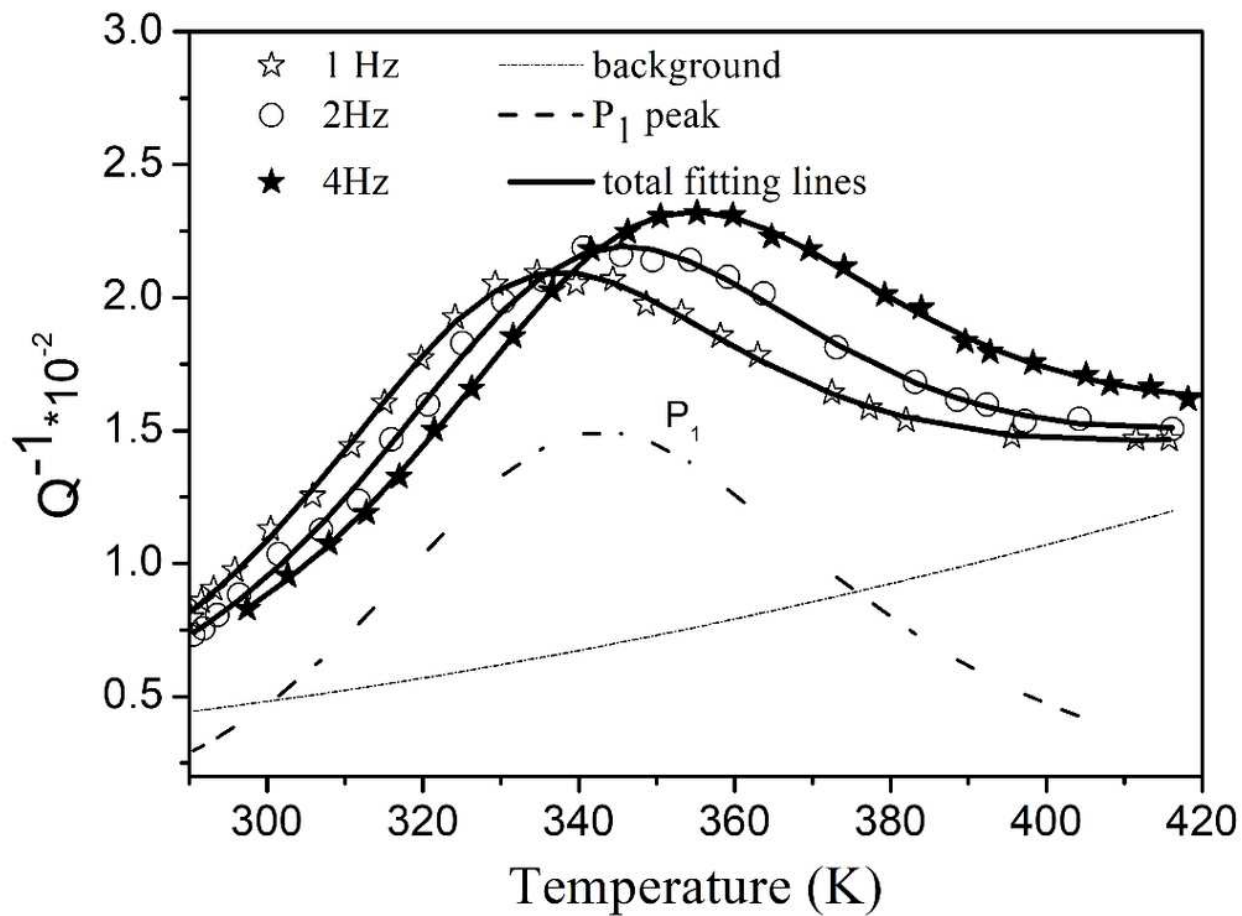


Figure 7

IF Q^{-1} versus temperature for the $\text{Na}_{0.52}\text{Bi}_{0.47}\text{Ti}_{0.985}\text{Ga}_{0.015}\text{O}_{3-\delta}$ sample measured at different frequencies (1 Hz, 2 Hz and 4 Hz) in the temperature range from 290 K to 425 K and non-linear fitting results.

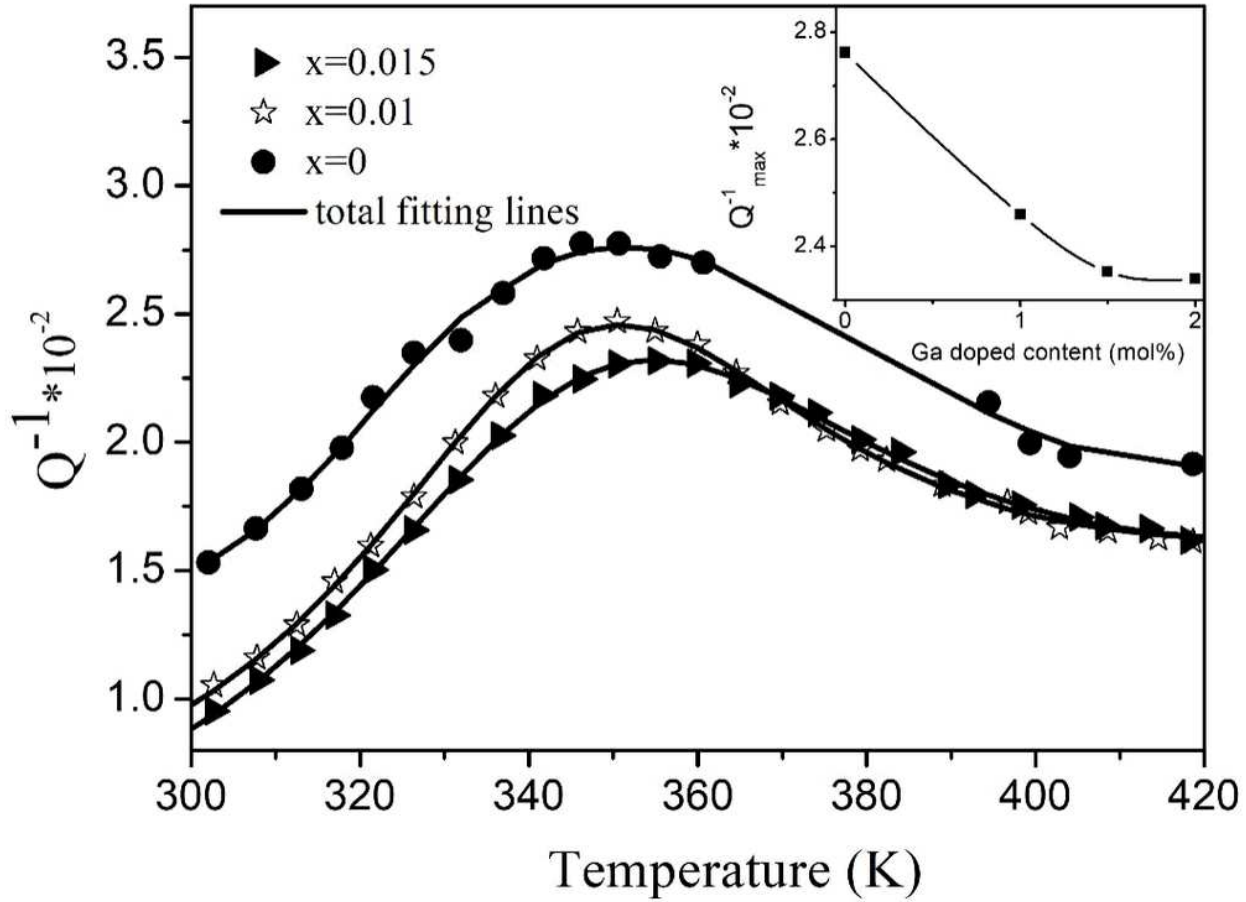


Figure 8

IF Q^{-1} versus temperature for the $\text{Na}_{0.52}\text{Bi}_{0.47}\text{Ti}_{1-x}\text{Ga}_x\text{O}_{3-\delta}$ ($x=0, 0.01, 0.015$) samples measured at 4 Hz in the temperature range from 290 K to 440 K. The curve of the relaxation time τ versus Ga^{3+} doped content is given in the inset.